



Studying the Passivity and Breakdown of Duplex Stainless Steels at Micrometer and Nanometer Scales – The Influence of Microstructure

Jinshan Pan*

Division of Surface and Corrosion Science, Department of Chemistry, KTH Royal Institute of Technology, Stockholm, Sweden

OPEN ACCESS

Edited by:

Guang-Ling Song,
Xiamen University, China

Reviewed by:

Changdong Gu,
Zhejiang University, China
Gloria Pena Uris,
University of Vigo, Spain

*Correspondence:

Jinshan Pan
jinshanp@kth.se

Specialty section:

This article was submitted to
Environmental Materials,
a section of the journal
Frontiers in Materials

Received: 25 October 2019

Accepted: 21 April 2020

Published: 15 May 2020

Citation:

Pan J (2020) Studying the Passivity and Breakdown of Duplex Stainless Steels at Micrometer and Nanometer Scales – The Influence of Microstructure. *Front. Mater.* 7:133. doi: 10.3389/fmats.2020.00133

Duplex stainless steels (DSSs) consist of ferrite and austenite phases with approximately equal volume fraction. They exhibit combined superior mechanical strength and corrosion resistance, therefore are increasingly used in various applications. However, under certain conditions, passivity breakdown may occur, leading to corrosion initiation, which is often related to weak points in the heterogeneous microstructure. To understand the influence of microstructure on the passivity and breakdown of DSSs requires local probing techniques that can be used *in situ*, so that corrosion initiation process can be correlated to the microstructure. Recent studies employing advanced scanning probe microscopy and synchrotron-based techniques, in combination with electrochemical measurements, have contributed to a deep understanding of the passive film, passivity breakdown, and corrosion initiation of DSSs, as well as the influence of microstructural and environmental factors. This mini review presents a short summary of recent literature focusing on the studies utilizing local probing techniques and synchrotron-based analyses.

Keywords: duplex stainless steel, microstructure, passive film, passivity breakdown, *in-situ*, local probing, synchrotron technique

INTRODUCTION

Duplex stainless steels (DSSs) contain ferrite and austenite phases with approximately equal volume fraction. They are increasingly used in many industrial applications due to their superior mechanical properties and corrosion resistance (Charles, 1991, 2007; Nilsson, 1992; Sedriks, 1996). There are lean (low alloyed) (Charles, 2015), standard (e.g., 2205), and super and hyper (high alloyed) DSS grades (Chai and Kangas, 2016). Their corrosion resistance depends strongly on the alloying elements, especially Cr, Mo, and N, which determine the pitting resistance (Nilsson, 1992; Sedriks, 1996; Charles, 2007; Chai and Kangas, 2016). Super DSS grades (e.g., 2507) and hyper DSS grades (e.g., 3207) have a pitting resistance equivalent number over 40 and around 50, respectively. Corrosion behavior of DSSs is complicated due to the presence of phase boundaries that are preferential

sites for precipitation of secondary phases/particles, and the partitioning of alloying elements, i.e., more Cr and Mo in ferrite, and more Ni and N in austenite (Combrade and Audouard, 1991; Olsson, 1995; Garfias-Mesias et al., 1996; Weber and Uggowitzner, 1998; Chai and Kangas, 2016). The type, size, and distribution of precipitate particles in the microstructure play a crucial role in the corrosion initiation (Alkire and Verhoff, 1998), and local interactions between the phases have an influence on the corrosion resistance (Combrade and Audouard, 1991; Olsson, 1995). Detailed knowledge of the microstructure, local electrochemical activities and corrosion processes occurring at micrometer and nanometer scales are needed to gain a fundamental understanding of the passivity and breakdown, and the corrosion resistance of DSSs, which is required for development of high performance stainless steels.

Traditionally, microstructure of alloys is characterized by using optical microscopy, scanning and transmission electron microscopy (SEM and TEM), energy dispersive spectroscopy (EDS), and X-ray diffraction (XRD). Corrosion behavior of the alloys in corrosive environments is evaluated by electrochemical measurements, e.g., potentiostatic/potentiodynamic polarization, and electrochemical impedance spectroscopy (EIS). Detailed information of the microstructure of DSSs can be obtained, however, traditional electrochemical measurements do not provide information of the local corrosion processes. Therefore, local probing techniques allowing *in-situ* measurements are needed to correlate the real time electrochemical information with the microstructure of the DSSs.

MICROSTRUCTURE AND PRECIPITATES

High levels of alloying elements are added to achieve excellent corrosion resistance and mechanical properties of DSSs. It is well-known that Cr is the key element for passive film formation, Ni enhances the passivity and balances the ferrite-austenite phase structure, Mo and N are added to strengthen the passivity and improve the resistance to localized corrosion and they have beneficial synergistic effects (Marcus, 2012). Microstructure of DSSs, e.g., grain size and austenite spacing, may vary due to heat treatment and processing. Because of high contents of the alloying elements, precipitation of secondary phases including intermetallics such as sigma and chi phases, as well as carbides and nitrides, can occur when DSSs are subjected to improper heat treatment and processing (Chan and Tjong, 2014; Paulraj and Garg, 2015). Generally, these precipitates have an adverse effect on the mechanical properties and the corrosion resistance due to depletion of alloying elements in the area adjacent to the precipitates (Nilsson, 1992; Chan and Tjong, 2014; Paulraj and Garg, 2015; Chai and Kangas, 2016). For example, precipitation of sigma phase rich in Cr and Mo leads to depletion of these alloying elements in the surrounding matrix, and precipitation of Cr nitrides causes depletion of Cr and N in the area adjacent to the particles (Chan and Tjong, 2014). However, under what conditions (e.g., location and size of sigma phase and Cr nitrides) these precipitates become detrimental are still unanswered questions.

LOCAL PROBING STUDIES USING STM/AFM

Local Probing Techniques

Different local electrochemical and microscopic techniques have been developed for *in-situ* corrosion studies, allowing characterization of metal-electrolyte interfaces while monitoring ongoing corrosion processes. Local probing techniques include microelectrode (Garfias-Mesias and Sykes, 1999), microcell (Kobayashi et al., 2000; Perren et al., 2001), local EIS (Annergren, 1996; Bayet et al., 1998), scanning vibration electrode technique (SVET) (Uchida et al., 2001), scanning reference technique (SRET) (Sargeant and Ronaldson, 1996; Lin et al., 1998), scanning tunneling microscopy (STM) (Fan and Bard, 1989; Miyasaka and Ogawa, 1990), atomic force microscopy (AFM) (Rynders et al., 1994; Reynaud-Laporte et al., 1997; Garfias-Mesias and Siconolfi, 2000; Williford et al., 2000), scanning electrochemical microscopy (SECM) (Zhu and Williams, 1997, 2000; Tanabe et al., 1998; Williams et al., 1998; Paik et al., 2000), scanning Kelvin probe (SKP) (Han and Mansfeld, 1997; Chen et al., 1998), and combination of these techniques (Böhni et al., 1995; de Wit et al., 1998; Guillaumin et al., 2001). Microelectrodes and microcells enable probing of small areas. SEVT and SRET techniques are capable to map local current or potential over the sample surface. STM and AFM can monitor topography changes with high spatial resolution. SECM detects local electrochemical activity at metal/electrolyte interfaces, whereas SKP measures Volta potential over metal surfaces in air or under a thin electrolyte film. These techniques have been employed for studying localized corrosion of metals and alloys, yielding valuable information. Examples of using local electrochemical techniques for corrosion studies are summarized in a recent review (Jadhav and Gelling, 2019). Different operation modes of STM and AFM have enabled *in-situ* characterization of metal surfaces and nanometer-scale mapping of local electrical, electrochemical, magnetic, and mechanical properties of the surfaces (Maurice and Marcus, 2018). For example, scanning Kelvin probe force microscopy (SKPFM) has been increasingly used in the studies of localized corrosion (Guillaumin et al., 2001; Rohwerder and Turcu, 2007), yielding relative nobility of microstructure components.

Ex-situ and *in-situ* STM/AFM Studies

Characterization of Phases in DSS and Their Relative Nobility

Volta potential mapping by SKPFM was employed firstly to evaluate relative nobility of ferrite and austenite phases in DSSs, showing several tens of mV difference in Volta potential between the two phases and also a potential drop at the phase boundary (Femenia et al., 2003). The austenite exhibited a nobler Volta potential than the ferrite, in agreement with a higher dissolution rate of the ferrite next to the austenite observed by *in-situ* STM measurements in chloride solutions. Later, magnetic force microscopy (MFM) was combined with SKPFM for characterization of the phases in DSSs including ferrite, austenite, sigma phase, and Cr nitrides (Sathirachinda et al., 2008, 2009, 2010, 2011). MFM maps revealed different magnetic

properties of the ferrite and austenite, allowing easy phase identification (Ramirez-Salgado et al., 2013). Combined MFM and SKPFM results provided information of the location of the precipitate particles and their corrosion tendency (Sathirachinda et al., 2008; Ramirez-Salgado et al., 2013). The high lateral resolution (better than 100 nm) of MFM and SKPFM enabled characterization of corrosion propensity of micro- and nano-meter sized precipitate particles and the surrounding matrix. A potential drop at the phase boundary was observed in slowly cooled 2205 DSS with sigma phase precipitate, and the depletion effects at the phase boundary were confirmed by Volta potential mapping and TEM/EDS analyses (Sathirachinda et al., 2009). Moreover, SKPFM study of 2507 DSS indicated that isothermally precipitated Cr nitrides (80–230 nm in size) at ferrite/austenite phase boundaries could be detrimental, whereas small quenched-in Cr nitrides (50–100 nm in size) formed inside the ferrite seemed to have small or no adverse effect on the corrosion behavior (Sathirachinda et al., 2010, 2011).

Influence of Microstructure on Localized Corrosion Initiation

Effect of nano-sized precipitate Cr nitrides in DSSs on their corrosion behavior was studied by electrochemical polarization and *in-situ* AFM measurements in 1M NaCl solution (Bettini et al., 2013, 2014). 2205 DSS exhibited a passive behavior despite of quenched-in Cr nitrides present in the ferrite, and preferential ferrite dissolution only occurred under transpassive conditions. At 50°C, selective austenite dissolution occurred, but the ferrite remained to be stable. The results show that finely dispersed quenched-in Cr nitrides in the ferrite do not cause localized corrosion, but elevated temperature can trigger localized corrosion initiation (Bettini et al., 2013). 2507 DSS at room temperature remained stable in a wide potential range of applied potential despite of presence of the Cr nitrides. At 90°C (above the critical pitting temperature), the isothermal Cr nitrides precipitated along the phase boundaries largely reduced the corrosion resistance of the austenite, while the small quenched-in Cr nitrides reduced the corrosion resistance slightly (Bettini et al., 2014). Moreover, the low Volta potential areas in weld fused zone were found to be preferential nucleation sites for pitting initiation of 2205 DSS (Sun et al., 2018). These *in-situ* local probing observations of DSSs with precipitated Cr nitride particles are in general agreement with the *ex-situ* SKPFM mapping of the relative nobility of the phases including the precipitates. However, the Volta potential measured at room temperature did not correlate to the corrosion behavior at elevated temperatures (Bettini et al., 2013, 2014).

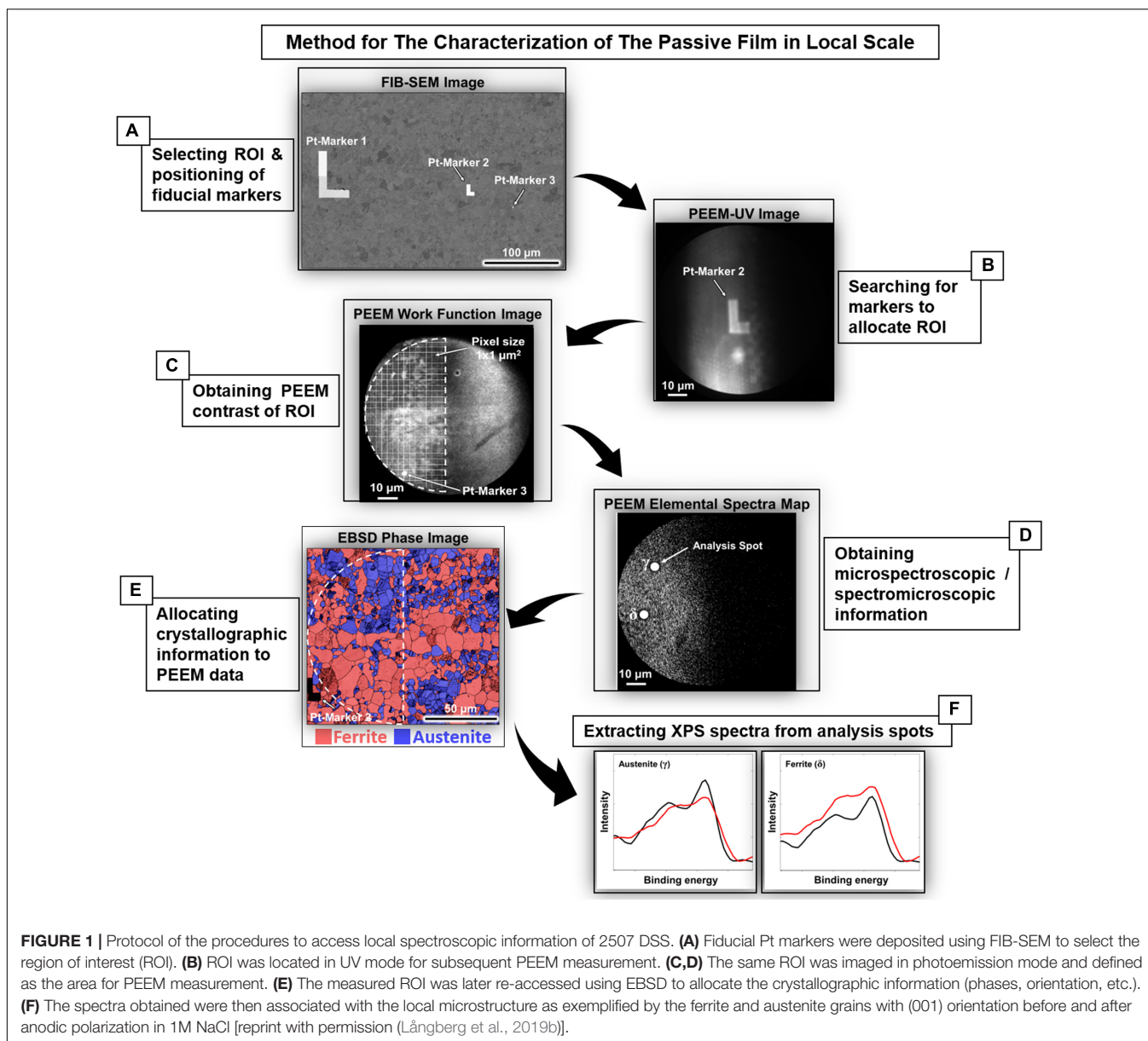
Influence of Heat Treatment, Mechanical Loading, and Hydrogen Charging

AFM/SKPFM/MFM have also been used for studies of other factors that affect corrosion behavior of DSSs. A study of the effect of annealing temperature on corrosion behavior of 2507 DSS showed that annealing at 1100°C resulted in a greater Volta potential difference between the two phases, with the austenite exhibited a higher Volta potential than the ferrite, in agreement with preferential dissolution of the ferrite in HCl

solution. Whereas, annealing at 1050°C led to a smaller Volta potential difference and a lower dissolution rate (Guo et al., 2011). SKPFM was used to investigate hydrogen-induced pitting corrosion of 2507 DSS. The hydrogen charging resulted in low potential areas at the ferrite/austenite boundaries, associated with pitting initiation. Different effects of hydrogen on ferrite and austenite were observed and attributed to different hydrogen behavior (solubility and diffusivity) in the two phases (Li et al., 2012; Guo et al., 2013a). *In-situ* SKPFM investigation of tensile deformation of 2205 DSS revealed that the slip bands generated by tensile deformation decrease the surface potential. The work function increased in the elastic deformation stage but decreased and stabilized in the plastic deformation stage (Wang et al., 2014). Combing electron back-scattering diffraction (EBSD) and SKPFM enabled correlation between Volta potential and strain localization in the microstructure of 2205 DSS, which facilitates the understanding of the influence of cold-work and heat treatment on the corrosion behavior (Örnek and Engelberg, 2015, 2016; Örnek et al., 2017). Furthermore, combining digital image correlation and SKPFM allowed *in-situ* study of effects of hydrogen and tensile strain on local Volta potential evolution and micro-deformation of 2507 DSS, providing information helpful for understanding the effects of microstructure and strain on hydrogen embrittlement of the DSS (Örnek et al., 2018b). Besides, a theoretical effort was made by first-principle calculations, showing that the difference in the properties between ferrite and austenite can be attributed to their electron work functions (Guo et al., 2016).

Probing Semiconducting Properties of Passive Film

Recently, current sensing AFM (CSAFM) was employed to investigate semiconducting properties of passive films on 2507 DSS. From the current maps, band-gap energies could be extracted from I-V curves obtained on the ferrite and austenite areas. The results showed that the conductivity of passive film on ferrite and austenite is different and decreases with increasing film formation potential that determines the film thickness and composition (Guo et al., 2013b, 2014). Hydrogen charging was found to significantly increase the conductivity of the passive film, which was higher on austenite than that on ferrite due to more hydrogen in austenite. Moreover, hydrogen charging caused an inversion of the conductivity from p-type to n-type. The highest passive film conductivity was seen at phase/grain boundaries, where pitting corrosion initiated (Guo et al., 2017; Yakubov et al., 2018). In some cases, I-V curves could be obtained through scanning tunneling spectroscopy (STS), the data provide similar information as CSAFM (Rahimi et al., 2019). Moreover, combined SKPFM and electrochemical measurements were used for characterization of passive films of DSS. Natural oxidation in air and chemical oxidation in concentrated nitric acid improved the nobility and reduced the Volta potential difference between ferrite and austenite, whereas hydrogen charging increased the Volta potential difference, resulting in a decreased nobility, more for ferrite than austenite (Örnek et al., 2019b).

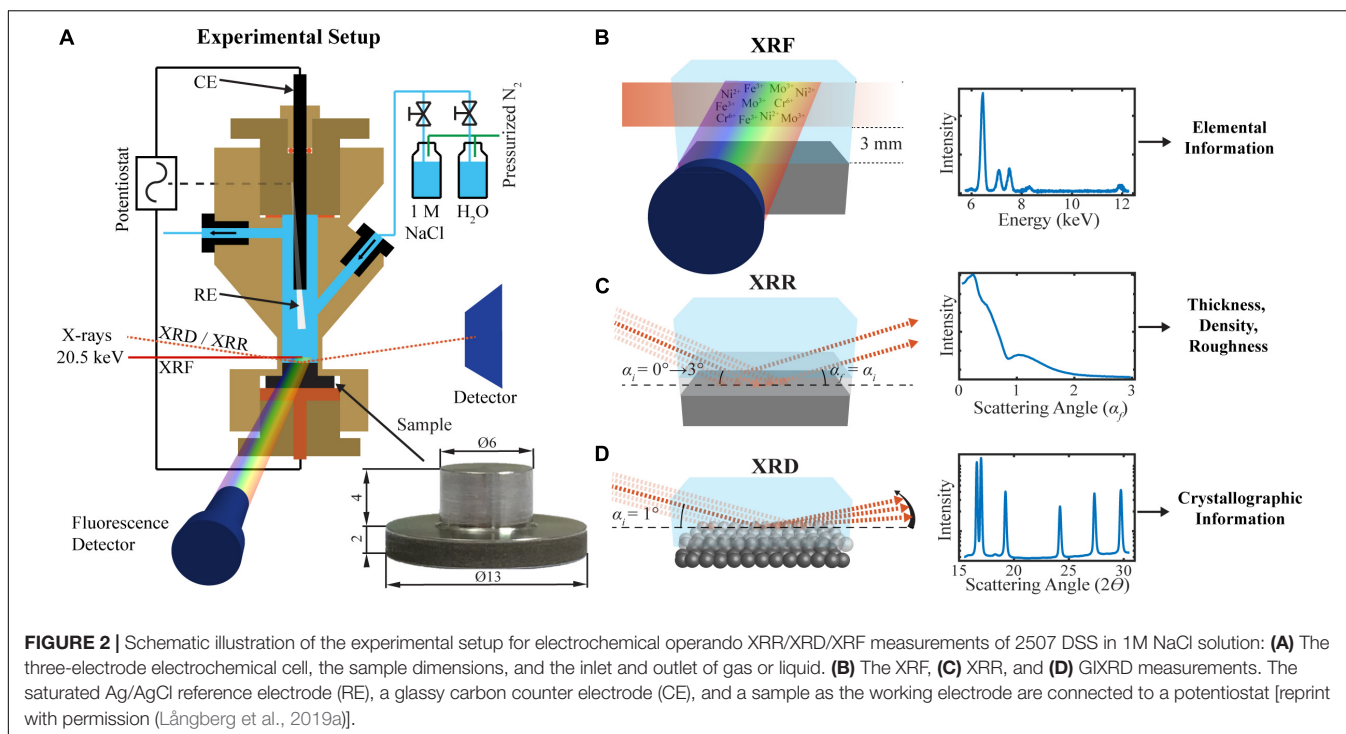


SURFACE ANALYSIS OF PASSIVE FILMS

Global Characterization of Passive Films

Passive films on metals have been studied extensively by using different analytical techniques (Strehblow, 2016; Maurice and Marcus, 2018). Both *ex-situ* chemical analysis techniques, e.g., X-ray photoelectron spectroscopy (XPS), Auger electron spectroscopy (AES), and *in-situ* microscopic techniques (AFM and STM), have been used for characterization of composition, structure and properties of the passive films. Synchrotron based X-ray diffraction (XRD) and absorption spectroscopy (XAS) have also been employed for *in-situ* analyses of the surface films (Virtanen et al., 2002; Monnier et al., 2014; Watanabe et al., 2015). XPS and AES were used to study passivation of 2205 DSS, focusing on lateral and depth distribution of Mo and

N in and near the passive layer. The passive film seemed to be homogeneous. The results showed Ni and N enrichment at the oxide/metal interface and also indications for Mo and N interaction both in and near the passive layer (Olsson and Hörnström, 1994; Olsson, 1995; Olsson and Landolt, 2003). Combined XPS analysis and electrochemical measurements of 2205 DSS showed that the passive film composition depends on pH of the solution and the polarization potential (Luo et al., 2011, 2012). For 2507 DSS, it was found that the passive film is composed of hydroxide and oxide of Fe and Cr, with Cr oxide close to the film/metal interface. Moreover, Cr enrichment and passive film growth occur upon increasing exposure temperature (Cui et al., 2017). By using angle-resolved XPS combined with electrochemical analyses, it was shown that the composition of the passive film formed on 2205 DSS in



borate buffer solutions varies with applied potential and exhibits n-type and p-type semiconductor character in different potential regions (Yao et al., 2019). The composition of passive film on 2205 DSS was substantially affected by hydrogen charging, which not only reduced the content of Cr_2O_3 , N and O^{2-} species inside the passive film, but also decreased its thickness (Luo et al., 2017).

Local Analysis of Passive Films

Due to intrinsic heterogeneous microstructure of DSSs, local analysis of the passive films is needed to assess local degradation of DSSs in corrosive environments. Different approaches have been used to gain local chemical information of passive films on individual phases. AES analysis during local ion sputtering provided elemental information of the surface layer with a lateral resolution of $5\ \mu\text{m}$ (Vignal et al., 2010, 2013), but no information about oxidation states of the elements. Selective etching of one phase and analyzing the remaining phase by XPS showed that the passive film composition is quite different on the two phases (Wang et al., 2015). However, the etching may have caused significant changes of the passive film. Further, single phase materials with chemical composition similar to the two phases in the DSS were analyzed by XPS, assuming that the passive film on the single phase is the same as that on the corresponding phase in the DSS (Gardin et al., 2018). This assumption is questionable because the chemical composition of the respective phases in the DSS depends on the processing and heat treatment, and the grain boundaries and residual strains may be different from the single phase due to different deformation and thermal expansion of the two phases. More suitable method is needed for local analysis of the passive films on DSSs.

Synchrotron X-Ray Analyses of Passivity and Passive Films

Analysis of Passive Films by X-Ray Photoemission Electron Microscopy

State-of-the-art synchrotron techniques enable microscopic chemical analysis of passive films on DSS without the need for sputtering, etching or use of single-phase materials. In a recent study, air-formed oxide and anodic passive film on 2507 DSS were analyzed by using hard X-ray photoemission electron microscopy (HAXPEEM) with lateral resolution of $1\ \mu\text{m}$. By varying the photon energy, information depth could be changed in order to probe different depths of the surface region. Pre-deposited Pt-markers in combination with EBSD allowed local analysis of the oxide film on individual grains of the ferrite and austenite, before and after electrochemical polarization (Långberg et al., 2019b). The measurement protocol showing the experimental procedures is displayed in **Figure 1**. Preliminary data analysis showed a certain difference in the composition (e.g., Cr_2O_3 content) of the surface films between the two phases, and, anodic polarization up to $1000\ \text{mV}/\text{Ag}/\text{AgCl}$ in $1\ \text{M}$ NaCl solution led to a growth of Cr- and Fe-oxides, diminishing of Cr-hydroxide, and an increased proportion of Fe^{3+} species (Långberg et al., 2019b).

Operando Synchrotron X-Ray Analyses of Passive Film and Passivity Breakdown

Passivity breakdown of highly-alloyed stainless steels is commonly believed to occur at a fixed potential (breakdown potential) due to further oxidation of Cr (III) in the passive film to soluble Cr (VI) species. However, the anodic current due to oxygen evolution at high potentials may be misleading in the interpretation of the measured polarization curves. In

a recent work, combined with electrochemical measurements, synchrotron-based X-ray reflectivity (XRR), X-ray fluorescence (XRF), and XRD were employed, in operando, to study the passivity and breakdown of 2507 DSS in 1M NaCl solution (Långberg et al., 2019a). Schematic illustration of the experimental setup is shown in **Figure 2**. Combined XRR, XRD, and XRF results revealed that the passivity breakdown is in fact a continuous degradation of the passive film over a certain potential range, accompanied by enhanced Fe dissolution before rapid Cr dissolution caused by increased potential. The breakdown process involves structural and compositional changes of both the passive film and the underlying alloy surface layer, as well as selective metal dissolution depending on the applied potential (Långberg et al., 2019a). The passivity breakdown of the 2507 DSS started to occur around 1000 mV/Ag/AgCl, and Fe dissolved more on the ferrite than the austenite. Upon further increasing potential, the passive film became thicker but less dense, while the underlying alloy surface layer became denser, indicating Ni and Mo enrichment, and rapid Cr dissolution occurred at ≥ 1300 mV/Ag/AgCl (Långberg et al., 2019a).

The grazing incidence XRD (GIXRD) provided structural information of the native oxide and anodic passive film on the 2507 DSS. The native oxide was composed of nano-crystalline mixed-oxides and hydroxides. Electrochemical polarization to higher potential in the passive region resulted in film thickening, preferential Fe dissolution, and partial loss of crystallinity (Örnek et al., 2018a). Comparing mechanically polished and electro-polished samples, the GIXRD results revealed that the surface strain induced by surface preparation has an influence on the passive film formation and evolution during anodic polarization. Specifically, surface strain affected crystallinity of the passive film, crystalline CrOOH diminished upon immersion in the NaCl solution, whereas crystalline FeOOH increased during anodic polarization in the passive potential range (Örnek et al., 2019a). Moreover, associated with metal dissolution, strain relaxation occurred in both austenite and ferrite grains during immersion in the solution. Polarization to transpassive regime led to maximum strain relaxation, and selective dissolution was significantly reduced due to large strains in the austenite (Örnek et al., 2019a).

CONCLUSION

DSSs possess intrinsic heterogeneous microstructure, and micro- or nanometer-sized particles of intermetallic phases, carbides

REFERENCES

- Alkire, R., and Verhoff, M. (1998). The bridge from nanoscale phenomena to microscopic processes. *Electrochim. Acta* 43, 2733–2741.
- Annergren, I. (1996). *Electrochemical Impedance Spectroscopy for In-Situ Studies of Anodic Dissolution and Pitting Corrosion of Iron-Chromium Alloys*. Doctoral thesis, Royal Institute of Technology, Stockholm.
- Bayet, E., Huet, F., Keddam, M., Ogle, K., and Takenouti, H. (1998). Adaptation of the scanning vibration electrode technique to AC mode: local electrochemical impedance measurement. *Mater. Sci. Forum* 57, 289–292.

and nitrides, etc., may form in the microstructure due to improper heat treatment and processing. *Ex-situ* and *in-situ* local probing techniques have been employed, in combination with electrochemical measurements, for characterization of the phases present in the microstructure and the composition, structure, and properties of the passive films. The microstructure components may lead to micro-galvanic effects, and the precipitate particles may cause depletion of alloying elements in the boundary regions, all have an influence on the corrosion susceptibility. Passive films on DSSs are composed of mixed oxides and hydroxides of mainly Cr and Fe, but also minor Mo-compounds. The thickness, composition, and structure of the passive film depend on the alloying contents and the formation conditions. The alloy surface layer underneath the passive film also plays an important role in the passivity. There are heterogeneities in the passive films of DSSs, which are related to the microstructure, while heat treatment, mechanical deformation, hydrogen charging, as well as pH and temperature of the aqueous media, all can alter the passive film. Weak sites of the passive film may trigger localized corrosion.

Combination of different *ex-situ* and *in-situ* local probing techniques provides complementary information about corrosion propensity and localized corrosion initiation, and enables the correlation with the microstructure. *In-situ* and operando measurements utilizing advanced synchrotron-based techniques yield fundamental understanding of structural, chemical and electrochemical processes, at nanometer or atomic scale, involved in the passivity and breakdown of DSSs.

AUTHOR CONTRIBUTIONS

JP wrote the manuscript.

FUNDING

Financial support by the Swedish Science Council (Vetenskapsrådet) through project Grants Nos. 2015-04490 and 2015-06092 was greatly acknowledged.

ACKNOWLEDGMENTS

I wish to thank the Ph.D. students, academic and industrial collaborators who have contributed to our own works on DSSs.

- Bettini, E., Kivisäkk, U., Leygraf, C., and Pan, J. (2013). Study of corrosion behavior of a 22% Cr duplex stainless steel: influence of nano-sized chromium nitrides and exposure temperature. *Electrochim. Acta* 113, 280–289.
- Bettini, E., Kivisäkk, U., Leygraf, C., and Pan, J. (2014). Study of corrosion behavior of a 2507 super duplex stainless steel: influence of quenched-in and isothermal chromium nitrides. *Intern. J. Electrochem.Soc.* 9, 61–80.
- Böhni, H., Suter, T., and Schreyer, A. (1995). Micro- and nanotechniques to study localized corrosion. *Electrochim. Acta* 40, 1361–1368.
- Chai, G., and Kangas, P. (2016). Super and hyper duplex stainless steels: structures, properties and applications. *Proc. Struct. Integ.* 2, 1755–1762.

- Chan, K.-W., and Tjong, S.-C. (2014). Effect of secondary phase precipitation on the corrosion behavior of duplex stainless steel. *Materials* 7, 5268–5304.
- Charles, J. (1991). "Super duplex stainless steel: structure and properties," in *Proceedings of the Duplex Stainless Steels '91, Conference*, Beaune.
- Charles, J. (2007). *Past, Present, and Future of Duplex Stainless Steels, Stainless Steel World 2007*. Maastricht: John Wiley & Sons.
- Charles, J. (2015). *Duplex Families and Applications: A Review, Part 3, The Lean Duplex Grades*. Maastricht: Stainless Steel World.
- Chen, C., Breslin, C. B., and Mansfeld, F. (1998). Scanning Kelvin probe analysis of the potential distribution under small drops of electrolyte. *Mater. Sci. Forum* 181, 289–292.
- Combrade, P., and Audouard, J.-P. (1991). "Duplex stainless steels and localized corrosion resistance," in *Proceedings of the Duplex Stainless Steels '91, Conference*, Beaune.
- Cui, Z. Y., Wang, L. W., Ni, H. T., Hao, W. K., Man, C., Chen, S. S., et al. (2017). Influence of temperature on the electrochemical and passivation behavior of 2507 duplex stainless steel in simulated desulfurized flue gas condensates. *Corros. Sci.* 118, 31–48.
- de Wit, J. H. W., van der Weijde, D. H., and de Jong, A. J. (1998). Local measurements in electrochemistry and corrosion technology. *Mater. Sci. Forum* 69, 289–292.
- Fan, F. R. F., and Bard, A. J. (1989). In-situ scanning tunneling microscopy study of the corrosion of type 304L stainless steel in aqueous chloride media. *J. Electrochem. Soc.* 136:166.
- Femenia, M., Canalias, C., Pan, J., and Leygraf, C. (2003). Scanning Kelvin probe force microscopy and magnetic force microscopy for characterization of duplex stainless steels. *J. Electrochem. Soc.* 150:B274.
- Gardin, E., Zanna, S., Seyeux, A., Allion-Maurer, A., and Marcus, P. (2018). Comparative study of the surface oxide films on lean duplex stainless steel and corresponding signal phase stainless steels by XPS and ToF-SIMS. *Corros. Sci.* 143, 403–413.
- Garfias-Mesias, L. F., and Siconolfi, D. J. (2000). In-situ high-resolution microscopy on duplex stainless steels. *J. Electrochem. Soc.* 147:2525.
- Garfias-Mesias, L. F., and Sykes, J. M. (1999). Metastable pitting in 25Cr duplex stainless steel. *Corros. Sci.* 41, 959–987.
- Garfias-Mesias, L. F., Sykes, J. M., and Tuck, C. D. S. (1996). The effect of phase composition on the pitting corrosion of 25Cr duplex stainless steel in chloride solutions. *Corros. Sci.* 38, 1319–1330.
- Guillaumin, V., Schmutz, P., and Frankel, G. (2001). Characterization of corrosion interfaces by the scanning kelvin probe force microscopy technique. *J. Electrochem. Soc.* 148:B163.
- Guo, L. Q., Bai, Y., Xu, B. Z., Pan, W., Li, J. X., and Qiao, L. J. (2013a). Effect of hydrogen on pitting susceptibility of 2507 duplex stainless steel. *Corros. Sci.* 70, 140–144.
- Guo, L. Q., Lin, M. C., Qiao, L. J., and Volinsky, A. A. (2013b). Ferrite and austenite phase identification in duplex stainless steel using SPM techniques. *Appl. Surf. Sci.* 287, 499–505.
- Guo, L. Q., Hua, G. M., Yang, B. J., Liu, H., Qiao, L. J., Yang, X. G., et al. (2016). Electron work functions of ferrite and austenite phases in a duplex stainless steel and their adhesive forces with AFM silicon probe. *Sci. Rep.* 6: 20660.
- Guo, L. Q., Li, M., Shi, X. L., Yan, Y., Li, X. Y., and Qiao, L. J. (2011). Effect of annealing temperature on the corrosion behavior of duplex stainless steel studied by in-situ techniques. *Corros. Sci.* 53, 3733–3741.
- Guo, L. Q., Lin, M. C., Qiao, L. J., and Volinsky, A. A. (2014). Duplex stainless steel passive film electrical properties studied by in-situ current sensing atomic force microscopy. *Corros. Sci.* 78, 55–62.
- Guo, L. Q., Qin, S. X., Yang, B. J., Liang, D., and Qiao, L. J. (2017). Effect of hydrogen on semiconductive properties of passive film on ferrite and austenite phases in a duplex stainless steel. *Sci. Rep.* 7:3317.
- Han, L. T., and Mansfeld, F. (1997). Scanning Kelvin probe analysis of welded stainless steel. *Corros. Sci.* 39, 199–202.
- Jadhav, N., and Gelling, V. J. (2019). Review-the use of localized electrochemical techniques for corrosion studies. *J. Electrochem. Soc.* 166: C3461.
- Kobayashi, Y., Virtanen, S., and Böhn, H. (2000). Microelectrochemical studies on the influence of Cr and Mo on nucleation events of pitting corrosion. *J. Electrochem. Soc.* 147, 155–159.
- Långberg, M., Örnek, C., Evertsson, J., Harlow, G. S., Linpé, W., Rullik, L., et al. (2019a). Redefining passivity breakdown of super duplex stainless steel by electrochemical operando synchrotron near surface X-ray analyses. *NPJ Mater. Degradat.* 3:22.
- Långberg, M., Örnek, C., Zhang, F., Cheng, J., Liu, M., Grånäs, E., et al. (2019b). Characterization of native oxide and passive film on austenite/ferrite phases of duplex stainless steel using synchrotron HAXPEEM. *J. Electrochem. Soc.* 166, C3336–C3340.
- Li, M., Guo, L. Q., Qiao, L. J., and Bai, Y. (2012). The mechanism of hydrogen-induced pitting corrosion in duplex stainless steel studied by SKPFM. *Corros. Sci.* 60, 76–82.
- Lin, C., Luo, J., Zhuo, X., and Tian, Z. (1998). Scanning microelectrode studies of early pitting corrosion of 18/8 stainless steel. *Corrosion* 54, 265–270.
- Luo, H., Dong, C. F., Li, X. G., and Xiao, K. (2012). The electrochemical behavior of 2205 duplex stainless steel in alkaline solutions with different pH in the presence of chloride. *Electrochim. Acta* 64, 211–232.
- Luo, H., Dong, C. F., Xiao, K., and Li, X. G. (2011). Characterization of passive film on 2205 duplex stainless steel in sodium thiosulphate solution. *Appl. Surf. Sci.* 258, 631–639.
- Luo, H., Li, Z. M., Chen, Y. H., Ponge, D., Rohwerder, M., and Raabe, D. (2017). Hydrogen effects on microstructural evolution and passive film characteristics of a duplex stainless steel. *Electrochem. Commun.* 79, 28–32.
- Marcus, P. (ed.) (2012). *Corrosion Mechanisms in Theory and Practice*, 3rd Edn. Boca Raton, FL: CRC Press.
- Maurice, V., and Marcus, P. (2018). Progress in corrosion science at atomic and nanometric scales. *Prog. Mater. Sci.* 95, 132–144.
- Miyasaka, A., and Ogawa, H. (1990). In-situ observation of a stainless steel surface in aqueous solutions using scanning tunneling microscopy. *Corros. Sci.* 31, 99–103.
- Monnier, J., Reguer, S., Foy, E., Testemale, D., Mirambet, F., Saheb, M., et al. (2014). XAS and XRD in situ characterization of reduction and reoxidation processes of iron corrosion products involved in atmospheric corrosion. *Corros. Sci.* 78, 293–303.
- Nilsson, J. O. (1992). Super duplex stainless steel. *Mater. Sci. and Tech.* 8:685.
- Olsson, C. O. A. (1995). The influence of nitrogen and molybdenum on passive films formed on the austenite-ferrite stainless steel 2205 studied by AES and XPS. *Corros. Sci.* 37, 467–479.
- Olsson, C. O. A., and Hörnström, S. E. (1994). The Lateral Homogeneity of Passive Films Formed on the Duplex Stainless Steel 2205 Investigated with AES and XPS, Paper no. 68, Duplex Stainless Steel' 94*. Glasgow, UK.
- Olsson, C. O. A., and Landolt, D. (2003). Passive films on stainless steels – chemistry, structure and growth. *Electrochim. Acta* 48, 1093–1104.
- Örnek, C., and Engelberg, D. L. (2015). SKPFM measured Volta potential correlated with strain localization in microstructure to understand corrosion susceptibility of cold-rolled grade 2205 duplex stainless steel. *Corros. Sci.* 99, 164–173.
- Örnek, C., and Engelberg, D. L. (2016). Correlative EBSD and SKPFM characterisation of microstructure development to assist determination of corrosion propensity in grade 2205 duplex stainless steel. *J. Mater. Sci.* 51, 1931–1948.
- Örnek, C., Långberg, M., Evertsson, J., Harlow, G., Linpé, W., Rullik, L., et al. (2018a). In-situ synchrotron GIXRD study of passive film evolution on duplex stainless steel in corrosive environment. *Corros. Sci.* 141, 18–21.
- Örnek, C., Långberg, M., Evertsson, J., Harlow, G., Linpé, W., Rullik, L., et al. (2019a). Influence of surface strain on passive film formation of duplex stainless steel and its degradation in corrosive environment. *J. Electrochem. Soc.* 166:C3071.
- Örnek, C., Leygraf, C., and Pan, J. (2019b). Passive film characterisation of duplex stainless steel using scanning Kelvin probe force microscopy in combination with electrochemical measurements. *NPJ Mater. Degradat.* 3:8.
- Örnek, C., Reccagni, P., Kivisäkk, U., Bettini, E., Engelberg, D. L., and Pan, J. (2018b). Hydrogen embrittlement of super duplex stainless steel - towards understanding the effects of microstructure and strain. *Intern. J. Hydrogen Energy* 43, 12543–12555.
- Örnek, C., Walton, J., Hashimoto, T., Ladwein, T. L., Lyon, S. B., and Engelberg, D. L. (2017). Characterisation of 475°C embrittlement of duplex stainless steel microstructure via scanning Kelvin probe force microscopy and magnetic force microscopy. *J. Electrochem. Soc.* 164, C207–C221.

- Paik, C. H., White, H. S., and Alkire, R.-C. (2000). Scanning electrochemical microscopy of dissolved sulfur species from inclusions in stainless steel. *J. Electrochem. Soc.* 147:4120.
- Paulraj, P., and Garg, R. (2015). Effect of intermetallic phases on the corrosion behavior and mechanical properties of duplex stainless steel and super-duplex stainless steel. *Adv. Sci. Technol. Res. J.* 9, 87–105.
- Perren, R. A., Suter, T. A., Uggowitzer, P. J., Weber, L., Magdowski, R., Böhni, H., et al. (2001). Corrosion resistance of super duplex stainless steels in chloride ion containing environments: investigations by means of a new microelectrochemical method I. precipitation-free states. *Corros. Sci.* 43, 707–745.
- Rahimi, E., Kosari, A., Hosseinpour, A., Davoodi, A., Zandbergen, H., and Mol, J. M. C. (2019). Characterization of the passive layer on ferrite and austenite phases of super duplex stainless steel. *Appl. Surf. Sci.* 496:143634.
- Ramirez-Salgado, J., Dominguez-Aguilar, M. A., Castro-Dominguez, B., Hernandez, P., and Newman, R. C. (2013). Detection of secondary phases in duplex stainless steel by magnetic force microscopy and scanning Kelvin probe force microscopy. *Mater. Character.* 86, 250.
- Reynaud-Laporte, L., Vayer, M., Kauffman, J. P., and Erre, R. (1997). An electrochemical-AFM study of the initiation of the pitting corrosion of a martensitic stainless steel. *Microsc. Microanal. Microstruct.* 8, 175–185.
- Rohwerder, M., and Turcu, F. (2007). High-resolution Kelvin probe microscopy in corrosion science: scanning Kelvin probe force microscopy (SKPFM) versus classical scanning Kelvin probe (SKP). *Electrochim. Acta* 53, 290–299.
- Rynders, R. M., Paik, C. H., Ke, R., and Alkire, R. C. (1994). Use of in-situ atomic force microscopy to image corrosion at inclusions. *J. Electrochem. Soc.* 141:1439.
- Sargeant, D. A., and Ronaldson, G. I. (1996). Quantitative measurements of localized corrosion using the scanning reference electrode technique on type 316 stainless steel. *Microsc. Anal.* 52, 21–32.
- Sathirachinda, N., Gubner, R., Pan, J., and Kivisäkk, U. (2008). Characterization of phases in duplex stainless steel by magnetic force microscopy/scanning Kelvin probe force microscopy. *Electrochim. Solid State Lett.* 11:C42.
- Sathirachinda, N., Pettersson, R., and Pan, J. (2009). Depletion effects at phase boundaries in 2205 duplex stainless steel characterized with SKPFM and TEM/EDS. *Corros. Sci.* 51, 1850–1860.
- Sathirachinda, N., Pettersson, R., Wessman, S., Kivisäkk, U., and Pan, J. (2011). SKPFM study of chromium nitrides in 2507 super duplex stainless steels – implications and limitations. *Electrochim. Acta* 56, 1792–1803.
- Sathirachinda, N., Pettersson, R., Wessman, S., and Pan, J. (2010). Study of nobility of chromium nitrides in isothermally aged duplex stainless steels by using SKPFM and SEM/EDS. *Corros. Sci.* 52, 179–184.
- Sedriks, A. J. (1996). *Corrosion of Stainless Steels*. Maastricht: John Wiley & Sons.
- Strehblow, H. H. (2016). Passivity of metals studied by surface analytical methods, a review. *Electrochim. Acta* 212, 630–654.
- Sun, J., Li, X., Sun, Y., Jiang, Y., and Li, J. (2018). A study on the pitting initiation of duplex stainless steel (DSS 2205) welded joints using SEM-EDS, SKPFM and electrochemistry methods. *Intern. J. Electrochem. Soc.* 13, 11607–11619.
- Tanabe, H., Togashi, K., Misawa, T., and Kamachi Mudali, U. (1998). In-situ pH measurements during localized corrosion of type 316LN stainless steel using scanning electrochemical microscopy. *J. Mater. Sci. Lett.* 17, 551–560.
- Uchida, H., Yamashita, M., Inoue, S., and Koterazawa, K. (2001). In-situ observation of crack nucleation and growth during stress corrosion by scanning electrode technique. *Mater. Sci. Forum* 496, 319–321.
- Vignal, V., Delrue, O., Heintz, O., and Peltier, J. (2010). Influence of the passive film properties and residual stresses on the micro-electrochemical behavior of duplex stainless steels. *Electrochim. Acta* 55, 7118–7729.
- Vignal, V., Krawiec, H., Heintz, O., and Mainy, D. (2013). Passive properties of lean duplex stainless steels after long-term aging in air studied by EBSD, AES, XRS, and local electrochemical impedance spectroscopy. *Corros. Sci.* 67:109.
- Virtanen, S., Schmuki, P., and Isaacs, H. S. (2002). In-situ X-ray absorption near edge structure studies of mechanisms of passivity. *Electrochim. Acta* 47, 3117–3125.
- Wang, R. J., Li, J. X., Su, Y. J., Qiao, L. J., and Volinsky, A. A. (2014). Changes of work function in different deformation stage for 2205 duplex stainless steel by SKPFM. *Proc. Mater. Sci.* 3, 1736–1741.
- Wang, Y., Cheng, X. Q., and Li, X. G. (2015). Electrochemical behavior and compositions of passive films formed on the constituent phases of duplex stainless steel without coupling. *Electrochem. Commun.* 57, 56–60.
- Watanabe, M., Yonezawa, T., Shobu, T., and Shoji, T. (2015). In situ X-ray diffraction measurement method for investigating the oxides films on austenitic stainless steel in simulated pressurized water reactor primary water. *Corrosion* 71, 1224–1236.
- Weber, L., and Uggowitzer, P. J. (1998). Partitioning of chromium and molybdenum in super duplex stainless steel with respect to nitrogen and nickel content. *Mater. Sci. Eng. A* 242:222.
- Williams, D. E., Mohiuddin, T. F., and Zhu, Y. (1998). Elucidation of trigger mechanism for pitting corrosion of stainless steels using submicron resolution scanning electrochemical and photoelectrochemical microscopy. *J. Electrochem. Soc.* 145:2664.
- Williford, R. E., Windisch, C. F. Jr., and Jones, R. H. (2000). In-situ observation of early stages of localized corrosion using the electrochemical atomic force microscope. *Mater. Sci. Eng. A* 288, 54–60.
- Yakubov, V., Lin, M. C., Volinsky, A. A., Qiao, L. J., and Guo, L. Q. (2018). The hydrogen-induced pitting corrosion mechanism in duplex stainless steel studied by current-sensing atomic force microscopy. *NPJ Mater. Degradat.* 2:39.
- Yao, J. Z., Macdonald, D. D., and Dong, C. F. (2019). Passive film on 2205 duplex stainless steel studied by photo-electrochemistry and ARXRS methods. *Corros. Sci.* 146:221.
- Zhu, Y., and Williams, D. E. (1997). Scanning electrochemical microscopic observation of a precursor state to pitting corrosion of stainless steel. *J. Electrochem. Soc.* 144, L43.
- Zhu, Y., and Williams, D. E. (2000). Explanation for initiation of pitting corrosion of stainless steels at sulfide inclusions. *J. Electrochem. Soc.* 147:1763.

Conflict of Interest: The author declares that the research was conducted in the absence of any commercial or financial relationships that could be construed as a potential conflict of interest.

Copyright © 2020 Pan. This is an open-access article distributed under the terms of the Creative Commons Attribution License (CC BY). The use, distribution or reproduction in other forums is permitted, provided the original author(s) and the copyright owner(s) are credited and that the original publication in this journal is cited, in accordance with accepted academic practice. No use, distribution or reproduction is permitted which does not comply with these terms.